# INFLUENCE OF SUSPENDED PARTICLES ON THE STRUCTURE OF A TURBULENT FLOW IN A TUBE

V. G. Kalmykov

UDC 532.526

The results of an experimental investigation into the dispersed flow of a system subject to negative pressure gradients are presented. The measurements were based on an optical time-of-flight method in a water channel, using polystyrene spheres as the solid phase. The average and pulsational characteristics of the dispersed flow were obtained in the boundary (wall) region and also in the center (core) of the flow. For zero pressure gradient the influence of the solid phase expressed itself as a reduction in the level of turbulence and an increase in the extent of the viscous sublayer, leading to a fall in the coefficient of friction. For a negative pressure gradient the pressure of the solid phase generated small-scale vortices, reduced the extent of the viscous sublayer, and hence increased the coefficient of surface friction.

## Introduction

It is well known that the presence of dense particles in suspension has a major effect on the structure of turbulent flows. In certain cases the introduction of a solid phase reduces the hydrodynamic resistance, and in other cases it has the reverse effect. Publications on the subject were listed in [1]. The study of dispersed flows has so far been mainly directed at the case of friction with a zero pressure gradient. However, during the passage of highly dispersed and multiphase flows through nozzles and channels between the blades of turbines and pumping installations, as well as in various other technical devices, boundary layers with considerable negative pressure gradients are created. A study of these flows is highly desirable in view of the fact that negative pressure gradients have a considerable influence on heat transfer, chemical reactions, and hydraulic resistance. In order to analyze these processes in a regular and soundly based manner, the accumulation of experimental data regarding the physical structure of such flows is a vital matter.

## 1. Experimental Method

Experiments were carried out in a hydraulic test installation comprising two open tanks connected by a stainless steel tube of square cross section having a side 40 mm long. At a distance of about 60 diameters from the inlet aperture of the tube an experimental Plexiglas section was installed. The inner surfaces of the experimental section were made flush with the inner surfaces of the tube walls. In order to create a longitudinal negative pressure gradient, a stainless steel plate $\Delta = 0.2$ mm thick and $L = 130$ mm long was placed in the working section; with the help of a micrometer screw this served to compress the flow.

The measurements were carried out by the optical time-of-flight method [2], based on the time required for the particles suspended in the test medium to traverse a specified distance (base of measurement). The instants at which the particles cross the end points of the base (distinguished optically in a specified part of the flow) are recorded by means of a photoelectric system. In contrast to the arrangement described earlier [2], in which the signal was distinguished by photographing the pulses, in the present investigation we used an arrangement with two photomultipliers and a frequency meter. Bias lighting of the flow was supplied by means of a narrow light beam, which was directed along the channel and was capable of being moved in a transverse direction. By means of the optical system the image of the region thus separated out was focused on a diaphragm containing two parallel slits. The distance between the slits, the height of the slits, and the magnification of the optical system were calculated in accordance with the recommendations of [2]. The light pulses from each slit were separated by means of a prism and transmitted to photomultipliers. The pulses reaching

Moscow. Translated from Zhurnal Prikladnoi Mekhaniki i Tekhnicheskoi Fiziki, No. 2, pp. 111-118, March-April, 1976. Original article submitted March 10, 1975.

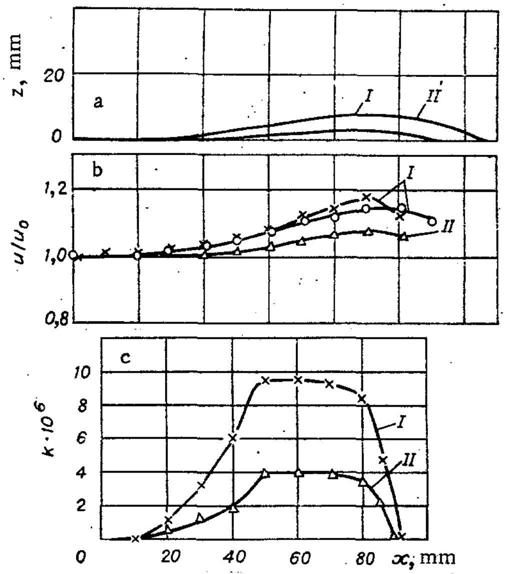


Fig. 1

the output of the photomultipliers, together with all the noise signals passing the amplifiers, were applied to the input of a discriminator. If the amplitude of the pulse exceeded the discrimination level, a rectangular pulse of specific amplitude and duration (independent of the parameters of the input signal pulses) was created at the output. The signals then passed to a frequency meter. The first pulse started the frequency meter and the second stopped it after a time corresponding to the time required for the particle to pass over the base distance. The spatial resolution in the direction of the objective axis was determined by the depth of focus of the objective and the slit width. If the particle moves away from the plane of sharpest focus, its image becomes blurred and the intensity of the light flux passing through the slits to the photomultipliers is reduced, i.e., there is a reduction in the amplitude of the pulse at the photomultiplier output. If the amplitude of this pulse falls below the set discrimination level, the particles are not recorded.

In order to check the method we measured the mean velocity profiles in the channel for several Reynolds number Re. The results of the measurements were compared with various power-law velocity distributions, in which the power indices n were selected from the measurements of Nikuradze [3]. The experimental data were in excellent agreement with a power-law velocity distribution in the channel. The measurements of the mean velocity close to the wall enabled us to determine the dynamic velocity from the slope of the mean velocity profile

$$u_* = (\nu du/dy)^{1/2}.$$

The values of the dynamic velocity thus obtained were compared with the values of $u_\tau$ calculated on the basis of the Blasius resistance law $\lambda = 0.316\mathrm{Re}^{1/4}$ and the expression for the tangential stress at the wall [3] $\tau_0 = \lambda\rho\bar{u}^2/8$. For the velocity profile measured with a zero pressure gradient, the values of $u_*$ calculated from the slope of the mean velocity profile were equal to 1.50 cm/sec, as compared with a value of $u_\tau$ = 1.475 cm/sec deduced from the Blasius formula.

It was shown in [4] that the velocity $u_*$ calculated from the slope of the profile close to the wall gives a more correct value of the stress at the wall, and that the velocity $v_*$ should be regarded as a matching constant which brings the experimental results into coincidence with the logarithmic part of the Klauser law.

## 2. Experimental Results

The positions of the plate required for creating high and medium pressure gradients (I and II) are shown in Fig. 1a, while Fig. 1b shows the mean velocity distribution along the axis of the channel for the corresponding pressure gradient (the crosses signify single-phase flow and the circles, dispersed flow; $\bar{d}$ = 0.82 mm). In the case of a high pressure gradient, as the dispersed medium moves the solid phase lags with respect to the main flow in the converger section, owing to the inertia of the particles. Up to a coordinate of x = 70 mm no difference appeared in the velocities of the single-phase and dispersed flows. As a pressure gradient parameter we used the quantity

$$k = -\frac{\nu}{\rho u_1^3}\frac{dp}{dx} = \frac{\nu}{u_1^2}\frac{du_1}{dx},$$

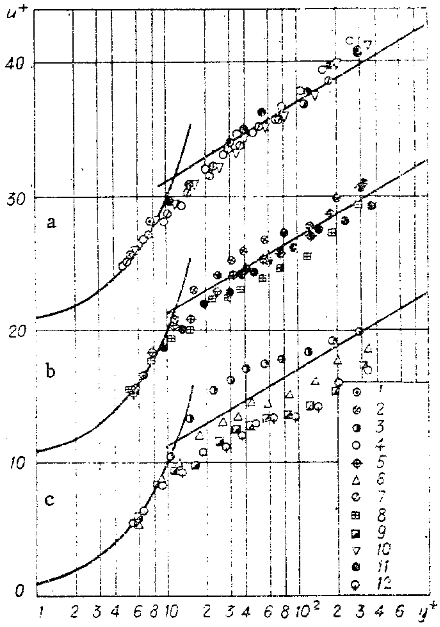


Fig. 2

which may be measured directly from experiment.

The distribution of the parameter k along the section under consideration is shown in Fig. 1c. The velocity profile was measured over the channel cross section at a point x = 60 mm from the starting point of the plate. For x values of 50-70 mm the parameter k remains practically constant. Experiments on single-phase and dispersed flows were carried out for three values of the parameter $k = 0$; $3.94 \cdot 10^{-6}$; and $9.42 \times 10^{-6}$. As solid phase we used polystyrene spheres with a concentration of 0.2 and 0.44 vol. % and two different diameters. The smaller diameter lay in the range $0.2 < d_1 < 0.44$ mm with a confidence probability $\alpha = 0.95$; the mean diameter was $\bar{d}_1 = 0.32$ mm. The larger diameter of the spheres (with the same confidence probability $\alpha$) lay within the range $0.66 < d_2 < 0.98$ mm having a mean value of $\bar{d}_2 = 0.82$ mm. The effective viscosity was calculated from the equation

$$\mu/\mu_0 = 1 + (5/2)c$$

(where c is the volumetric concentration of the solid phase), which is valid for low concentrations. This equation was used for determining the dynamic velocity.

The measured values of the average velocity were expressed in dimensionless coordinates $u^+ = u/u_*$ and $y^+ = yu_*/\nu$. Figure 2a-c illustrates the mean velocity profiles for three values of the parameter $k = 0$; $3.94 \cdot 10^{-6}$; and $9.42 \cdot 10^{-6}$, respectively. Points 1-3 correspond to single-phase flow; points 4-6, to dispersed flow with $\bar{d}_1 = 0.32$ mm and c = 0.2%; points 7-9, to dispersed flow with $\bar{d}_1 = 0.32$ mm and c = 0.44%; and points 10-12, to dispersed flow with $\bar{d}_2 = 0.82$ mm and c = 0.2%.

The Reynolds numbers based on the equivalent diameter of the cross section x = 60 mm respectively equaled 12,500, 13,000, and 11,580. Let us consider the case of the motion of single-phase and dispersed flows under a zero pressure gradient k = 0. We see by considering the results presented in Fig. 2a that the particle concentration and diameter have no effect on the velocity profile at the wall. A slight deviation of the velocity distribution in the center of the tube from the Klauser law $u^+ = 5.75 \lg y^+ + 5.5$ results from the fact that (in contrast to the tube) the outer region of the turbulent boundary layer borders the incident flow striking the plate, and this flow has a very low turbulence compared with the layer itself. The values of the dimensionless velocity on the channel axis $u_1^+ = u_1/u_*$ are somewhat lower for a single-phase flow than the values of the velocity $u_1^+$ obtained for a dispersed flow, this is a result of the slight reduction in resistance which occurs on introducing the solid phase. We remember that the coefficient of surface friction $c_f = 2(u_1^+)^{-2}$.

In order to analyze the structure of the flow in the central part of the channel we constructed profiles of the velocity defect (difference) $(u_1 - u)/u_*$ (Fig. 3). For k = 0 the particle size and concentration have no influence on the law of velocity distribution in the channel. The law governing the velocity difference

$$(u_1 - u)/u_* = 5.75 \lg \delta/y$$

only gives a satisfactory representation of the velocity profile in the outer part of the turbulent boundary layer

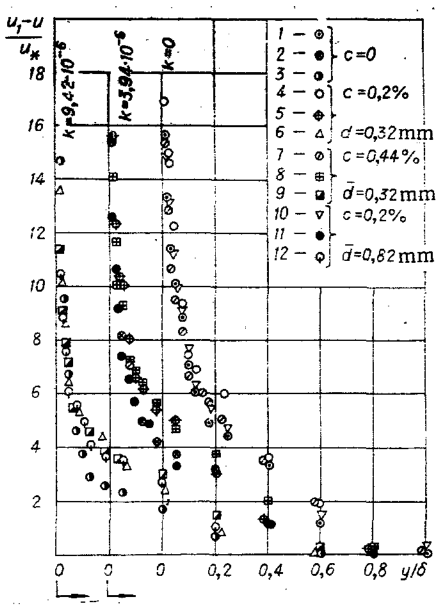


Fig. 3

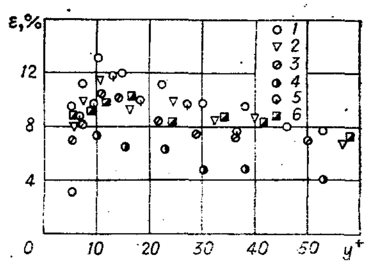


Fig. 4

for values of $y/\delta > 0.5$. The deviation from this law in the region close to the wall is the greater, the smaller the Reynolds number. The reduction in the intensity of the turbulence on introducing the solid phase is confirmed by the experimental data presented in Fig. 4 (case 1, single-phase flow; 2, dispersed flow with $c = 0.2\%$ and $\bar{d} = 0.82$ mm; 3, dispersed flow with $c = 0.44\%$ and $\bar{d} = 0.32$ mm).

An analysis of the oscillograms representing the velocity pulsations confirms our assertion regarding the influence of the solid phase on the characteristics of the turbulent flow. Figure 5a contains the oscillograms of the velocity pulsations at a distance of $y = 0.35$ mm from the wall for single-phase and dispersed flows (1 and 2, respectively) subject to a zero pressure gradient. The time interval between the marks is 0.02 sec. We see that the influence of the solid phase appears as a reduction in the turbulent pulsations. A qualitative model for the reduction in the hydraulic resistance of turbulent flows which occurs after introducing small amounts of suspended impurity into a liquid was proposed in [5]. It was shown that for low concentrations the reduction in the hydraulic resistance increased with increasing c and d.

Let us now consider the motion of single-phase and dispersed flows in the presence of a longitudinal pressure gradient. It is well known that for a negative pressure gradient the viscous sublayer of a single-phase flow increases, while the velocity pulsations in the boundary layer diminish. Under certain conditions the turbulent boundary layer may become laminar. In our experiments the thickness of the viscous sublayer $y_L^+$ increased from 6-7 to 14 on increasing the pressure gradient k from 0 to $9.42 \cdot 10^{-6}$ (Fig. 2a, c). However, despite the presence of this severe negative pressure gradient, no transition from turbulent to laminar flow occurred, evidently because of the considerable degree of turbulence of the main flow, which amounted to ~4-5%.

The reduction in the level of the turbulent pulsations may be seen by comparing the oscillograms (Fig. 5a, b, 1–1) and the intensities of the turbulence (Fig. 4, cases 1 and 4).

The introduction of the solid phase into the turbulent flow in the presence of a negative pressure gradient affects the characteristics in a manner differing substantially from the case of zero pressure gradient. First, the existence of the solid phase reduces the thickness of the viscous sublayer, since the particles penetrate into the latter and turbulize it. Thus, whereas for a single-phase flow the laminar sublayer $y_L^+ \simeq 14$, for $c = 0.2\%$, $y_L^+ \simeq 8-9$, and for $c = 0.44\%$, $y_L^+ \simeq 6$ (Fig. 2c).

As regards its influence on the average velocity profile, an increase in the particle diameter is probably equivalent to an increase in the concentration of smaller particles, since the larger particles penetrate more effectively into the viscous sublayer.

Outside the viscous sublayer the influence of the dispersed particles in the presence of a negative pressure gradient appears as a displacement of the mean velocity profile plotted in semilogarithmic coordinates, and the law corresponding to the wall may be written in the form

$$u^+ = (1/\varkappa)\ln y^+ + c,$$

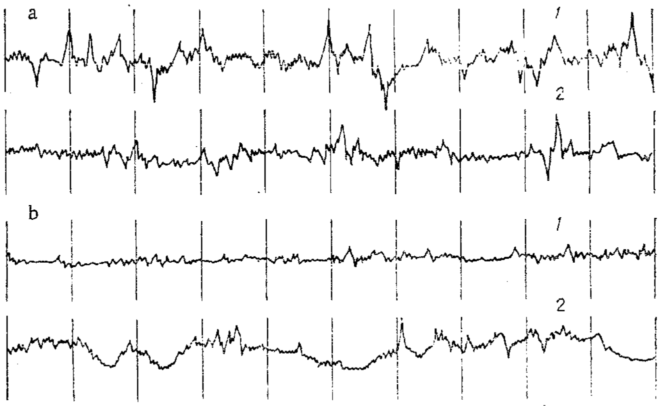


Fig. 5

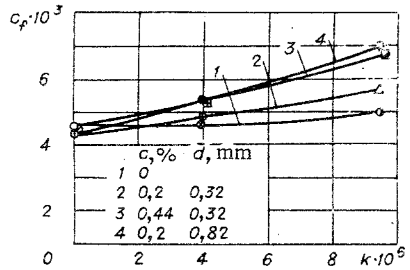


Fig. 6

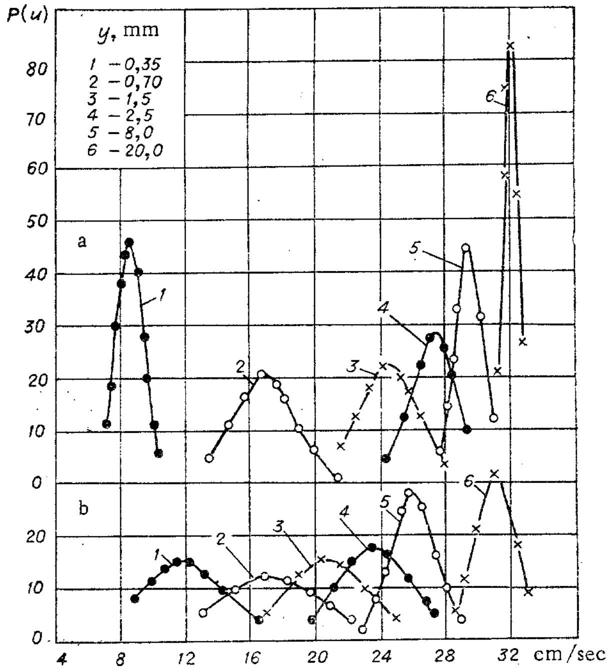


Fig. 7

where c is a constant of integration, depending on the parameter k, the diameter of the spheres, and the concentration of the solid phase. In the dispersed flow the deviation in the mean velocity profile $u^+ = f(y^+)$ takes place in the opposite direction to the case of the single-phase flow, the more so the greater the diameter and concentration of the particles.

The reduction in the velocity $u_1^+$ on the channel axis is a result of the increase in surface friction. Figure 6 shows the coefficients of surface friction for the modes of flow under consideration.

The presence of a negative pressure gradient results in a deformation of the velocity defect (difference) profile, with a simultaneous layering of the profiles for both single-phase and dispersed flows (Fig. 3). With increasing pressure gradient the quantity $(u_1 - u)/u_*$ diminishes for corresponding coordinates.

The increase in the hydraulic resistance of the dispersed flow by comparison with the single-phase flow may be explained by the fact that the solid particles not only disrupt the turbulent modes but also generate small vortices themselves. A consideration of the experimental data regarding turbulence intensities in the cross section of the boundary layer (cases 4-6) and the oscillograms representing the velocity pulsations close to the wall at a coordinate y = 0.35 mm (Fig. 5b) confirm this conclusion.

In the present investigation, by statistically analyzing the experimental results, we calculated the probability density distribution of the velocity in the boundary layer at various distances from the wall, using the equation

$$P(u) = (2\pi)^{-1/2}\sigma^{-1} \exp\{-(u - \bar{u})^2/2\sigma^2\},$$

where $\sigma$ is the mean square deviation and $\bar{u}$ is the average velocity.

The results of the measurements were checked in relation to the normal velocity distribution law on the basis of the $\chi^2$ criterion. A comparison between the calculated $\chi^2$ values and the critical values obtained for the corresponding degrees of freedom shows that there are no grounds for doubting the normality of the velocity distribution in the boundary layer.

Figure 7a and b illustrate the probability density distribution $P(u)$ of the velocity in the boundary layer in the presence of a negative pressure gradient ($k = 9.42 \cdot 10^{-6}$) for single-phase and dispersed flows, respectively ($c = 0.2\%$, $\bar{d} = 0.82$ mm). We see that, on introducing the dispersed particles, the viscous sublayer is turbulized, and the mean flow velocity $\bar{u}$ at coordinate $y = 0.35$ mm increases from 8.6 to 11.8 cm/sec, i.e., by a factor of almost 1.36 times, with a simultaneous increase in the intensity of the turbulence from 3.2 to 8.7%. However, beginning at a distance of $y \geq 1.0$ mm from the wall, the velocity of the dispersed flow diminishes by comparison with the single-phase flow for the corresponding coordinates, this being a consequence of the increase in the hydraulic resistance.

The author wishes to thank Yu. A. Buevich for interest in this work and V. L. Zalukaev for participation in the experiments.

## LITERATURE CITED

1. S.-T. Hsu, Hydrodynamics of Multiphase Systems [Russian translation], Mir, Moscow (1971).
2. G. R. Baranova, "Development of an optical time-of-flight method for measuring the mean velocity and degree of turbulence, and its application to the study of high-temperature, high-velocity flows," Candidate's Dissertation, Moscow (1970).
3. H. Schlichting, Boundary Layer Theory, 6th ed., McGraw-Hill (1968).
4. S. Klein, W. Reynolds, F. Schraub, and P. Ranstadler, "Structure of turbulent boundary layers," in: Mekhanika [Periodic Collection of Translations of Foreign Articles], No. 4, (1969), pp. 41-78.
5. Yu. A. Buevich, "Model for the fall in resistance encountered on introducing particles into a turbulent flow of viscous liquid," Izv. Akad. Nauk SSSR, Mekh. Zhidk. Gaza, No. 2, 114-120 (1970).